ULTRA-DOWNSIZING OF INTERNAL COMBUSTION ENGINES

V. Gheorghiu

HAW Hamburg University of Applied Sciences, Germany

E-mail: victor.gheorghiu@haw-hamburg.de

Abstract   The downsizing of internal combustion engines (**ICE**) is already recognized as a very suitable method for the concurrent enhancement of indicated fuel conversion efficiency (**IFCE**) and the lowering of CO_2 and NO_x emissions [1], [2]. In this report, **ultra-downsizing** is introduced as an even higher stage of development of ICE. Ultra-downsizing will be implemented here by means of real Atkinson cycles using asymmetrical crank mechanisms, combined with multi-stage high-pressure turbocharging and very intensive intercooling. This will allow an increase of ICE performance while keeping the thermal and mechanical strain strength of engine components within the current usual limits.

1. Introduction

The scarcity of oil and gas reserves and the global warming phenomenon both urge the automotive industry towards a decrease in fuel consumption and thus a reduction in CO2 emissions. These factors will also determine the future R&D trends for ICE.

Downsizing of ICE means simultaneous decreasing the displaced volume (usually by reducing the number of cylinders) and increasing the indicated mean pressure (**IMEP**) by means of turbocharging [1], [2]. This allows the preservation of power and torque performance while decreasing the engine size. As a result, a) the mechanical and thermal losses are reduced, b) the engine becomes lighter, leading to a drop in the overall weight of the vehicle, and c) the engine operates more within its optimum fuel consumption zone. The advantages offered by a) and b) hold true even for ICE used in hybrid propulsion systems, while the advantage c) is already a feature of full-hybrid vehicles.

The level of downsizing determines the strength of the thermal and mechanical strains of engine components. In order to avoid exceeding the usual limits, either the boost pressure or the volumetric compression ratio (**VCR**) must be reduced accordingly. As a consequence, the whole potential of downsizing is not achieved and the IFCE and IMEP remain at a low level.

The current ICEs have classical (symmetrical) crank mechanisms (i.e. compression and expansion strokes of equal length) and follow the Seiliger cycles. Real implemented Atkinson cycles require unequal strokes featuring a shorter compression stroke, which leads to a higher IFCE [3], [5]. Atkinson cycles have been used so far mostly with symmetrical crank mechanisms, where the intake valves are closed very late in the cycle [3] [4], [5]. Thus, a part of the charge sucked into the cylinder is pushed back to the intake pipes, and the effective compression stroke is decreased. This quasi implementation of Atkinson cycles shows no noticeable improvements of the IFCE and, hence, it will not be discussed in the course of this paper (see [3] and [5] for details).

Real Atkinson cycles can be implemented only with the help of asymmetrical crank mechanisms. This allows using concurrently very high boost pressures (to increase the IMEP) and higher VCR (to enhance the IFCE) and to set them much more independently of each other compared to Seiliger cycles [3], [5]. As an important part of the fresh charge compression takes place beyond the cylinder, the high compressed fresh charge can be cooled intensively before it is sucked into the cylinder. The following moderate compression in the cylinder (i.e. with relative lower VCR) leads to lower temperature peaks during the combustion process and, consequently, to less NOx emissions.

This approach has already been proved in several previous theoretical investigations based on ideal Seiliger and Atkinson cycles [3], [5]. These investigations did not take into consideration the effect of heat exchange and frictional losses on the cycle in order to make it easier to check the solution and to draw a comparison between the Seiliger and Atkinson cycles. The performances achieved for IFCE and IMEP using this method are therefore unrealistically high and serve only as a general indication [3, 5].

This Paper expands on the previous investigations from [3, 5] to real Atkinson cycles by using the simulation tool BOOST (AVL Co). This tool allows consideration of the true geometrical dimensions of the engine components (cylinder, valves, channels, pipes, manifolds, turbocharger, intercooler, silencer etc.) and the losses caused by friction and heat transfer along the intake and exhaust gas pipes. In addition, the power balance of turbochargers determines the actual boost pressure level of the engine.

The turbochargers (**TC**) are modeled for these investigations in a simple manner. It describes the expansion process in the turbines (**Tx**) by means of their discharge coefficients while the air compaction in the compressors occurs up to a maximum pressure ratio which depends on the available turbine output. To be able to simulate cycles with very high boost pressures as well, three intercooled TC are placed in line (three-stage turbocharging, see Fig. 1). When the boost pressure required for preserving the pressure limit on the cycle is low, the superfluous TC are kept for simplicity and comparability in use (i.e. are not bypassed). In this case the expansion and compression ratios of the turbines and compressors tend gradually toward 1, i.e. these TC switch off themselves thermodynamically.
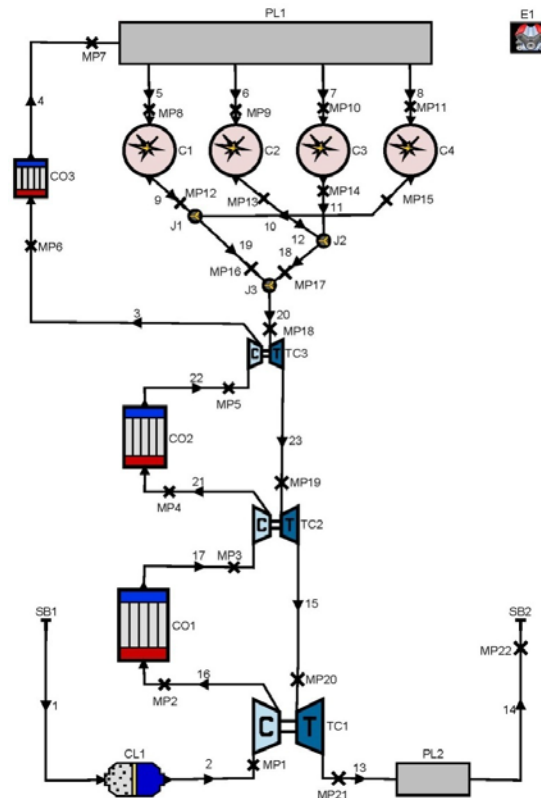
Figure 1 BOOST model of a four cylinder TC engine. Simple number denotes pipes, **Cx** = cylinder, **COx** = cooler, **TCx** = turbochargers, **PLx** = plenum, **Jx** = junctions, **CLx** = cleaner, **SBx** = system boundaries, **Ex** = engine and **MPx** = measuring points

The asymmetrical crank mechanism used here can realize classical piston displacements for the Seiliger as well as for the Atkinson cycles with various asymmetries between the compression and expansion strokes (see. Fig. 2A) and enable the variation of the VCR (see Fig. 2B).

As previously mentioned, the expansion and compression strokes are identical in the case of the Seiliger cycle. The limitation of the maximum pressure during the cycle determines the pair of parameters VCR - boost pressure. If a relatively high boost pressure is desired, the VCR must be reduced accordingly in order to accomplish the maximum pressure limitation on the cycle. This will also decrease the IFCE since it is determined primarily by the VCR. Furthermore, the expansion in the cylinder occurs largely incomplete and the exhaust gases exit the cylinder with still too high specific enthalpy, which decreases the IFCE even further. However, the expansion of exhaust gases in the turbines with its high specific enthalpy can only be used partly for driving the compressors and, therefore, for enhancing the boost pressure because it exceeds the pressure upper limit during the cycle.
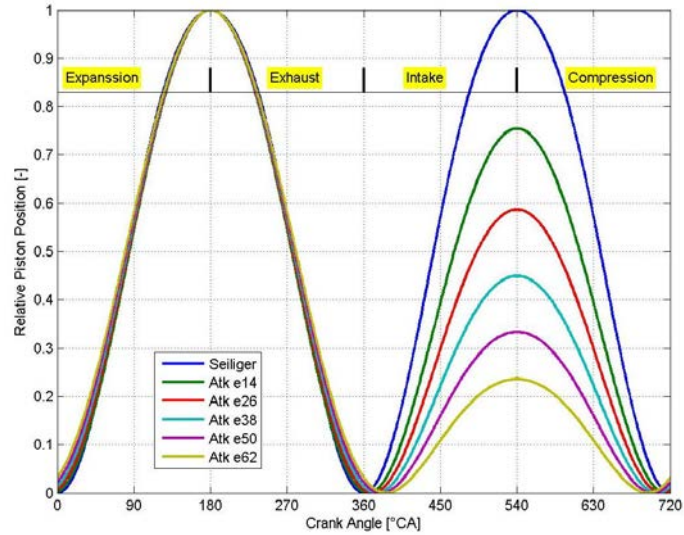
Figure 2A Relative displacements of the asymmetrical crank mechanism used in the **IC A**. The Atkinson (**Atk**) cycles are implemented by means of varying the eccentric radiuses **exx** of the crank mechanism used. The Seiliger cycle is realized with zero eccentric radius.
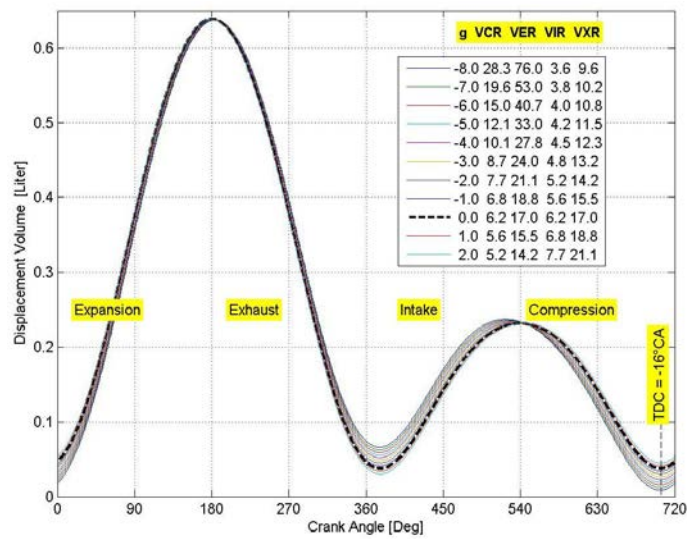

Figure 2B Displacement volume of the asymmetrical crank mechanism used in the **IC B**. The Atkinson (**Atk**) cycles are implemented by means of varying the parameter **g** of the crank mechanism used. The dashed curve represents the null position where a) expansion and exhaust and b) intake and compression strokes are identical.

The following facts can be used to summarize the current situation:

To raise the IFCE, most of the working gas expansion should occur within the cylinder. If, however, the expansion process occurs entirely within the cylinder (ideally, a full expansion occurs up to the ambient pressure), no additional boost pressure can be generated.

In order to increase the expansion part within the cylinder, the crank mechanism must provide a higher VER, which makes a long expansion stroke (and, therefore, an engine with a long piston displacement) necessary. However, that leads to high IFCE but quite low indicated specific power (kW/L) and IMEP of the engine.

For the simultaneously rising of the IFCE and the IMEP, the engine must be turbocharged and the ratio between the expansions within the cylinder and within the turbines (i.e. between internal and external expansion) must be optimized. To be able to optimize this ratio (i.e. between internal and external expansions) regardless of VCR, an asymmetrical crank mechanism is required in order to implement real Atkinson cycles.

2.   Investigation cases

The simulations in this Paper are carried out in the following two investigation cases (IC):

In the **IC A**, the simulated variants are based on a steady VER and a varied VCR. This means that identical expansion and exhaust strokes are kept unchanged and the identical intake and compression strokes are varied significantly - by means of varying the eccentric radiuses **exx** of the crank mechanism used - to allow the modification of the ratio between internal and external expansion. Some variants of the asymmetrical piston displacement are displayed in Fig. 2A.

In the **IC B**, the simulated variants are based on a steady eccentric radius (**e32**) where VER, VCR, volumetric intake ratio (**VIR**) and volumetric exhaust ratio (**VXR**) are varied simultaneously by means of the parameter **g**. Eleven variants of the asymmetrical piston displacement are displayed in Fig. 2B.

The goal of this Paper is to look for the optimum ratio between internal and external expansion, which leads simultaneously to maximizing the IFCE and enabling sufficiently high values of IMEP.

2.1. Setting of the simulations for both IC

The simulations of the piston displacements presented in Fig. 2A are carried out using the BOOST model from Fig. 1. The parameters and the performance of seven cycles are shown in Table 1. Many of the parameters from all cycles are kept identical in order to make comparison easier.

Most parameters of the BOOST model are selected for a hypothetical engine and are kept <u>unchanged</u> for all simulations. This includes parameters such as all geometrical dimensions (with the exception of the crank mechanism), valve timing, wall temperatures (300 K) and heat transfer coefficients (Re-analogy) of the pipes, as well as efficiencies and pressure losses of the intercoolers (target efficiency = 0.75, target pressure drop = 5 kPa) and friction coefficients in the pipes (0.019). Likewise, the efficiency of the turbochargers (compressor efficiency = 0.75, turbocharger overall efficiency = 0.5), as well as the blow by gap size of the cylinder, frictional characteristic curve of the engine and AFR - the combustion parameter (see Table 1A) - are also included.

A simple Vibe function is selected in order to model the combustion process. The different positions of the TDC in the Atkinson and Seiliger cycles (see Fig. 2 and 5) are compensated by choosing a suitable start of combustion (**SOC**), so that combustion begins in all cycles uniformly at 15°CA before TDC.

The various parameters from Table 1A for the IC A and from the Fig. 10B for the IC B are selected for the purpose of obtaining roughly the same maximum cylinder pressure **max(p) ≈ 230 bar** in all cycles. In order to reach this state, the discharge coefficients of the three turbines (μ_{T1}, μ_{T2} and μ_{T3}) are varied according to a) the influence of the back pressure behind the cylinder (e.g. at the measuring point MP12 for cylinder 1; see Fig. 1) and of b) the boost pressure (e.g. at MP8 for cylinder 1). In order to reach approximately the same expansion rate in all three turbines, their discharge coefficients are set at the same level and compensated with the cross sections ratios of the turbine output pipes. Hence, only the discharge coefficient of the third turbine μ_{T3} is adapted for each cycle to meet the cylinder peak pressure limit, since this sets the level of the other two discharge coefficients μ_{T2} and μ_{T1} (see Table 1A and Fig. 10B).

2.2. Simulation results and trends for IC A

After analyzing the performance based on the values presented in Table 1A, a host of trends becomes clear. For example:

All Atkinson cycles show better IFCE values than the Seiliger cycles (see also Fig. 5A). However, the Seiliger cycles reach higher IMEP values because of the longer intake stroke and, therefore, larger gas mass sucked in (see Fig. 9A). Furthermore, higher boost pressures p_{MP8} are required in both Atkinson and Seiliger

cycles in order to hold the parameter **max(p)** steady when VCR is reduced (see Table 1A).

Cycle	VER	VCR	μ_{T1}	μ_{T2}	μ_{T3}	n	AFR	SOC	CD	m_{Vibe}
	-	-	-	-	-	rpm	kg/kg	°CA	°CA	-
Atk e14	27,0	20,6	0,480	0,258	0,161	3000	14,6	-21	86	1,5
Atk e26	27,0	16,2	0,430	0,231	0,144	3000	14,6	-24	86	1,5
Atk e38	27,0	12,7	0,335	0,180	0,112	3000	14,6	-30	86	1,5
Atk e50	27,0	9,7	0,256	0,138	0,086	3000	14,6	-36	86	1,5
Atk e62	27,0	7,1	0,199	0,106	0,067	3000	14,6	-42	86	1,5
Seiliger	7,0	7,0	0,330	0,177	0,111	3000	14,6	-15	86	1,5
Seiliger	15,0	15,0	0,620	0,333	0,208	3000	14,6	-15	86	1,5

Cycle	VER	VCR	IFCE	IMEP	max(p)	max(T)	p_{MP8}	T_{MP8}	p_{MP12}	T_{MP12}
	-	-	-	bar	bar	K	bar	K	bar	K
Atk e14	27,0	20,6	0,419	25,7	231	2209	3,02	336	2,79	867
Atk e26	27,0	16,2	0,423	28,2	234	2197	4,08	343	3,78	877
Atk e38	27,0	12,7	0,423	27,9	237	2182	5,13	346	4,79	877
Atk e50	27,0	9,7	0,413	26,7	235	2167	6,55	348	6,16	913
Atk e62	27,0	7,1	0,391	24,6	229	2152	8,78	356	8,07	915
Seiliger	7,0	7,0	0,301	57,9	232	2292	12,48	450	15,85	1396
Seiliger	15,0	15,0	0,383	42,1	232	2344	4,62	361	4,62	1127

Table 1A Parameter (top) and Performance (bottom) for **IC A**. This table shows the **VER** (volumetric expansion ratio), **VCR** (volumetric compression ratio), μ_{Tx} (turbine discharge coefficients), **n** (engine speed), **AFR** (air-fuel ratio), **SOC** (start of combustion), **CD** (combustion duration), m_{Vibe} (exponent of Vibe function for cylinder heat release modeling), **IFCE** (indicated fuel conversion efficiency), **IMEP** (indicated mean pressure), **max(p)** and **max(T)** (maximum pressure and temperature during the cycle), p_{MP8} and T_{MP8} (mean boost pressure and temperature; i.e. at the measuring point MP8, see Fig. 1) and p_{MP12} and T_{MP12} (mean exhaust back pressure and temperature; i.e. at MP12, see Fig. 1) for cylinder 1.

The comparison of the **Atk e62** (with VCR = 7.1) and **Seiliger** (with VCR = 7) cycles shows that a) the Atkinson cycle has a 30% higher IFCE and reaches 58% less IMEP and b) the Seiliger cycle needs a 30% **higher** boost pressure (p_{MP8} in Table 1A) and must overcome a 50% higher cylinder back pressure - i.e. before T3 (p_{MP12} in Table 1A).

Moreover, the comparison of the **Atk e38 & e26** (with VCR = 12.7 respective = 16.2) and **Seiliger** (with VCR = 15) cycles shows that the Atkinson cycles have a 10% higher IFCE (although the maximum cylinder temperature **max(T)** is ca. 160 K, i.e. 7% lower) and 34% less IMEP.

The highest IFCE value for Atkinson cycles is not reached in the variant with the highest VCR, but in the variant where the VCR is about 50% of VER. Consequently, the optimum variant features an intake stroke equal to approx. 50% of the expansion stroke.

Some diagrams are introduced and analyzed below in order to determine the cause of these trends. The pressure-volume (**p,V**) diagrams of all cycles and pres-

sure-specific volume (**p,v**) diagrams of the intake and exhaust gas paths (for cylinder 1) are presented in Fig. 3A and 4A.
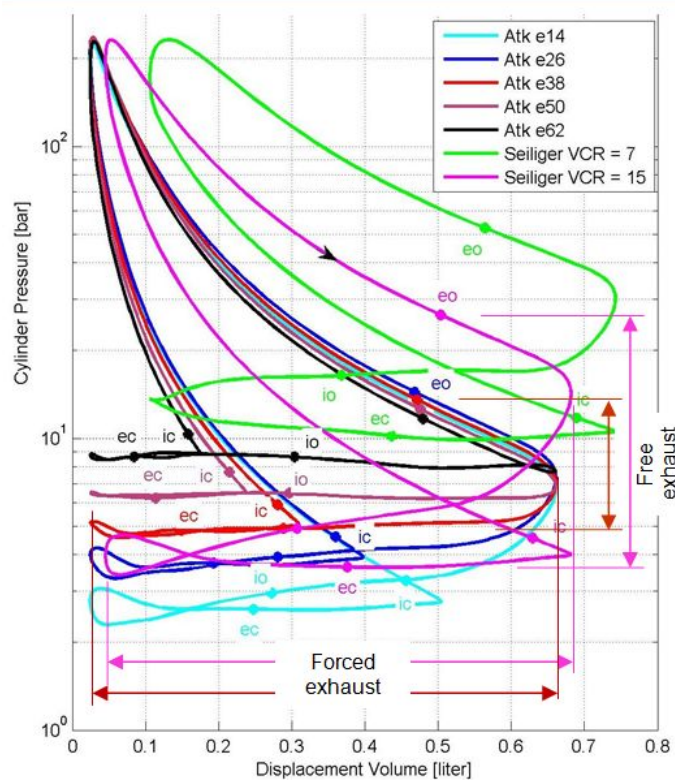

Figure 3A Cylinder pressure (logarithmic) - displacement volume (**p,V**) diagrams with valves timing for all cycles. Here **eo** denotes exhaust open, **ec** exhaust closed, **io** intake open, **ic** intake closed. The differences between the free and forced exhaust parts can be clearly observed. The forced exhaust diminishes IFCE as shown in Fig. 5A.

It can be inferred from Table 1A, as well as recognized in Fig. 3A and 4A, that the Seiliger cycle with VCR = 7 needs the highest boost pressure to reach the desired **max(p) ≈ 230** bar (because of its low VCR). The consequences are an extremely high back pressure p_{MP12} and falling ISFC because of the very intensive exhaust work required to push the exhaust gases out of the cylinder (see green curves up to **ec** points in Fig. 3A, 4A and 5A). Therefore, this cycle occurs exclusively in the pressure range above 10 bar (see Fig. 3A). For Atkinson cycle **Atk e38**, this situation is reversed (see Table 1A and Fig. 3A, 4A and 5A for comparison). This cycle occurs exclusively in the pressure range above 5 bar (see Fig. 3A).

The differences between both cycles can be clearly seen in the intake and exhaust gas paths. Fig. 4A and 7A show the three-stage compression of the air and all states after passing through each compressor and intercooler (with associated pressure losses). Fig. 4A and 8A show the three-stage expansion of the exhaust gases in the turbines. Fig. 8A shows, the discharge coefficients are properly adapted between the turbines because the expansion occurs almost linearly in all three stages.
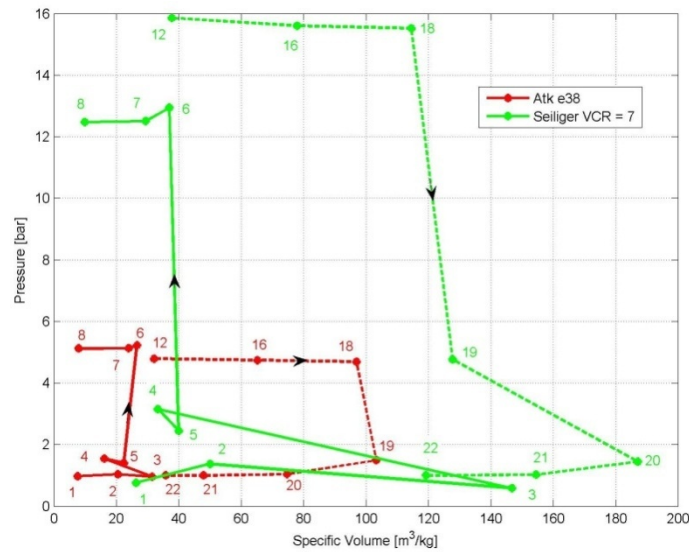

Figure 4A Pressure - specific volume (p,v) diagrams for some MP from the intake (solid lines) and exhaust (dashed lines) pipes for two selected cycles. The numbers denote the states of measuring points from Fig. 1.

The air compression and the exhaust gas expansion for the cycle **Atk e38** occur mostly in **TC3** (see Fig. 4A, 7A and 8A) because the exhaust gas pressure at the MP18 point (i.e. before **T3**, see Fig. 4A and 8A) is too low (see also Table 1A) to be able to adequately drive **T2** and **T1**. Consequently, the exhaust gases compress partly in **T2** and **T1** instead of expanding (see MP19 to MP21 in Fig. 4A). No modification of the IFCE sequence between variants is obtained by deleting **TC1** from the BOOST model (i.e. there is no need to remove the unnecessary **TC** in these simulations).

In all Atkinson cycles, the sucked intake gas mass changes minimally (see the red circle area on the left side of Fig. 9A), i.e. IMEP follows preponderantly IFCE variation and is, for the most part, independent of the boost pressure (p_{MP8}) variation.
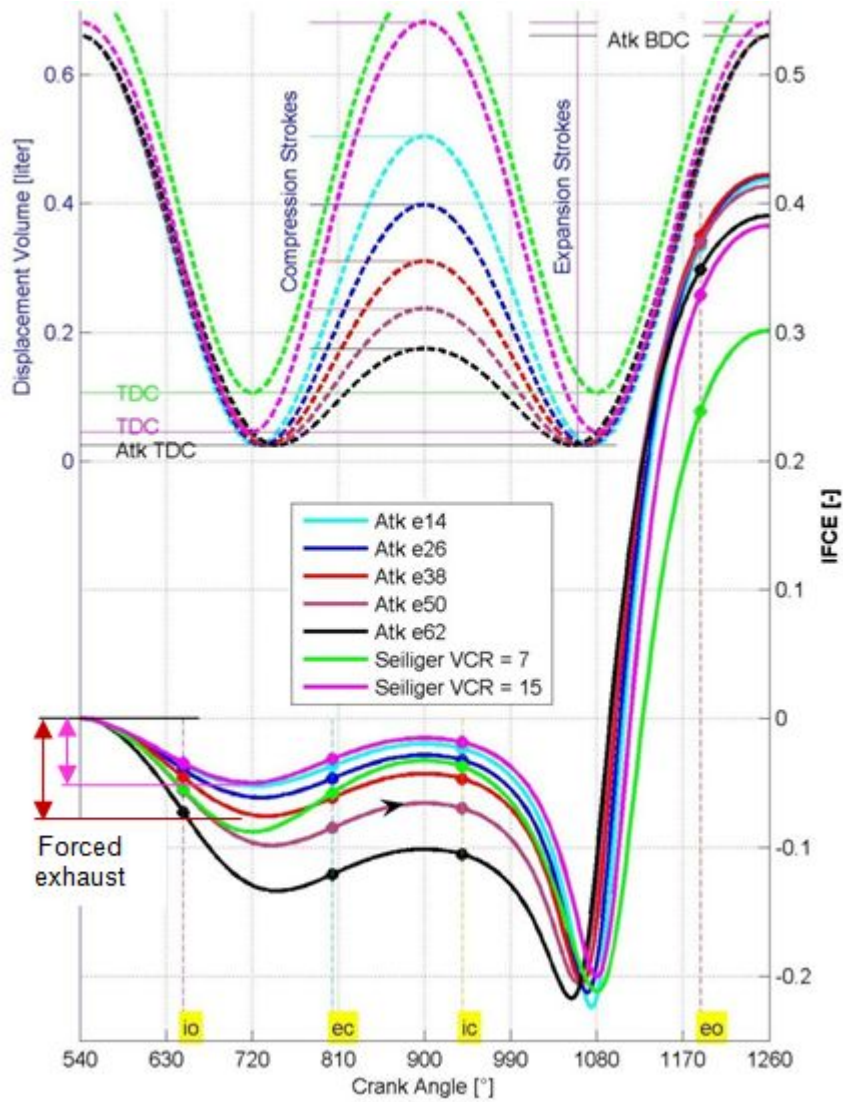
Figure 5A IFCE - crank angle (**IFCE,CA**) with valves timing (left axis) and displacement vol-
ume - crank angle (**V,CA**) diagrams for all cycles. The TDC top dead center and BDC bottom
dead center are shown here. The forced exhaust diminishes IFCE cycle-dependent.
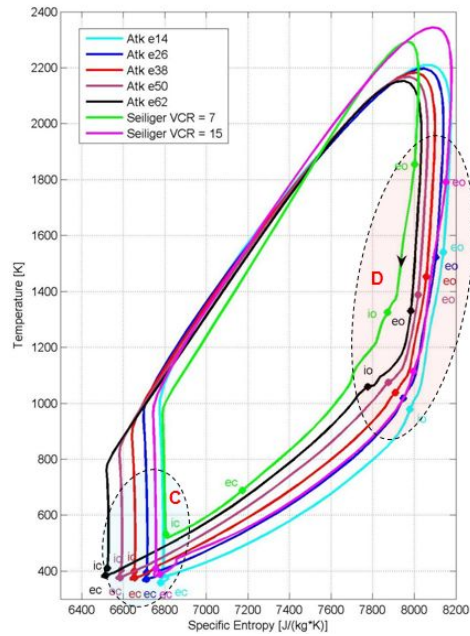
Figure 6A Temperature - specific entropy (T,s) diagrams with valves timing for all cycles. Details **C** and **D** are presented in expanded form in Fig. 7 and 8
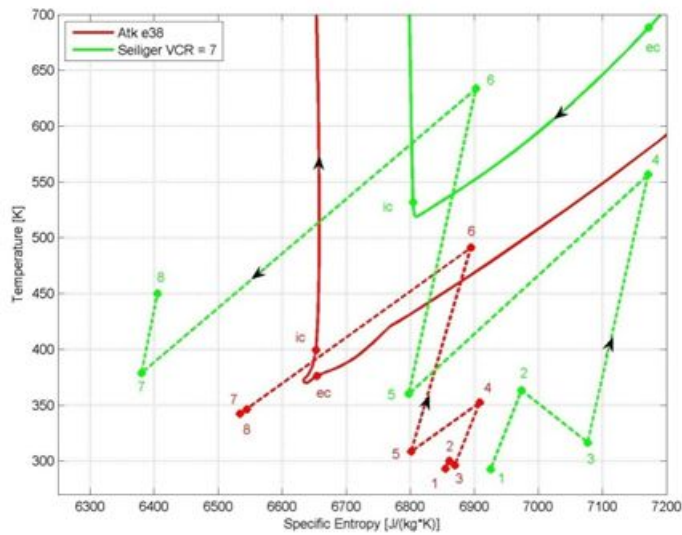

Figure 7A Temperature - specific entropy (T,s) diagrams for some MP (see Fig. 1) from intake pipes (dashed lines) superposed on **C** Detail of Fig. 6 (solid lines) for two selected cycles
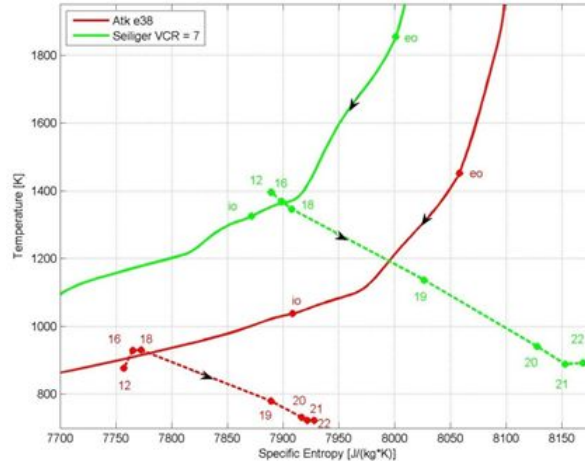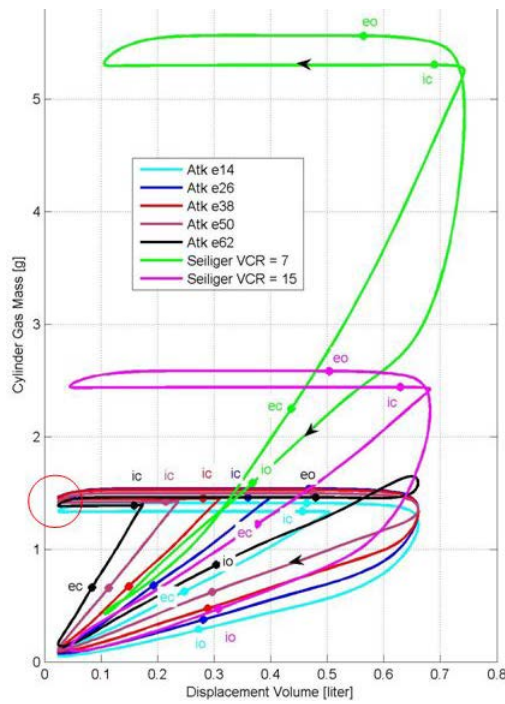
Figure 8A Temperature - specific entropy (**T,s**) diagrams for some MP (see Fig. 1) from exhaust pipes (dashed lines) superposed on **D** detail of Fig. 6 (solid lines) for two selected cycles

Figure 9A Gas mass - displacement volume (**m,V**) diagrams with valve timing for all cycles

2.3. Simulation results and trends for IC B

A number of trends becomes clear after analyzing the parameter and performances presented in Fig. 10B. For example:

This type of crank mechanism – which permits VCR variation (in this case via parameter **g**) – enables the implementation of Atkinson cycles for part and full-load operating points (**OPs**), where IMEP varies between 8.5 and 42 bar, even with stoichiometric AFR and without throttling.

Moreover, IFCE in all these OPs only varies within a 6% wide band (related to its maximum, see also Fig. 11B and 13B).

In all these OPs, the maximum cylinder pressure remains at approx. 230 bar and the maximum cylinder temperature varies between 1800 and 2300 K (see Fig. 12B and 13B). The optimization of the heat release could significantly reduce the maximum cylinder temperature (see [3], [5]).

In variant **g+2** (see legend), the maximum boost pressure (p_{PM8}) reaches nearly 12 bar, while the boost temperature (T_{PM8}) does not exceed 360 K (see Fig. 10B). In this case, the cylinder is filled to maximum (see Fig. 14B).

As a result of the extended expansion within the cylinder (see Fig. 10B) the exhaust gas temperatures before turbine **T3** (T_{MP12}) only reach a maximum of 1000 K. A benefit is that the turbine wheel must not be protected (e.g. by making the mixture leaner) against a higher gas temperature, while a disadvantage is that a higher exhaust gas pressure is required before **T3** (p_{MP12}) in order to achieve the desired boost pressure (p_{MP8}).

The required higher exhaust gas pressure before **T3** (p_{MP12}) (i.e. the cylinder back pressure) significantly diminishes the level of IFCE (i.e. by approx. 25%, see IFCE variation in Fig. 11B between 540°CA and **ec** position). The load independence of these IFCE losses is quite unexpected, but if the difference between cylinder pressure at **eo** and back pressure (p_{MP12}) in Fig. 12B is noted, the positive effect of the exhaust gases released from the cylinder (i.e. of the free exhaust) becomes evident. An additional optimization of valve timing can considerably reduce the back pressure and, therefore, these IFCE losses.

The residual gas concentration decreases, while VXR and boost pressure increase (see Fig. 10B). The increase in VXR makes the cylinder exhaust more complete (see Fig. 12B) and the increase in boost pressure favors the scavenging of residual gases from the cylinder.

The IMEP enhancement – from 8.5 to 42 bar, while AFR remains unchanged (stoichiometric) and IFCE only varies within a 6% wide band – is the result of the increase of aspirated gas mass into the cylinder (see Fig. 14B).
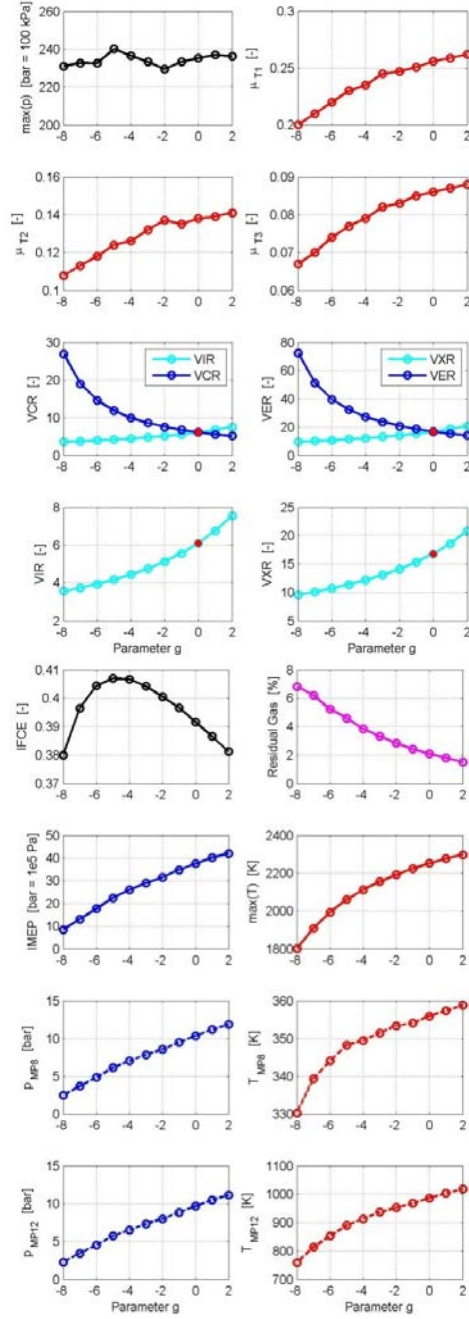
14

Figure 10B Parameter (top) and performance (bottom) for **IC B**. The parameters displayed have the same meaning as shown in Table 1A and Fig. 2B.
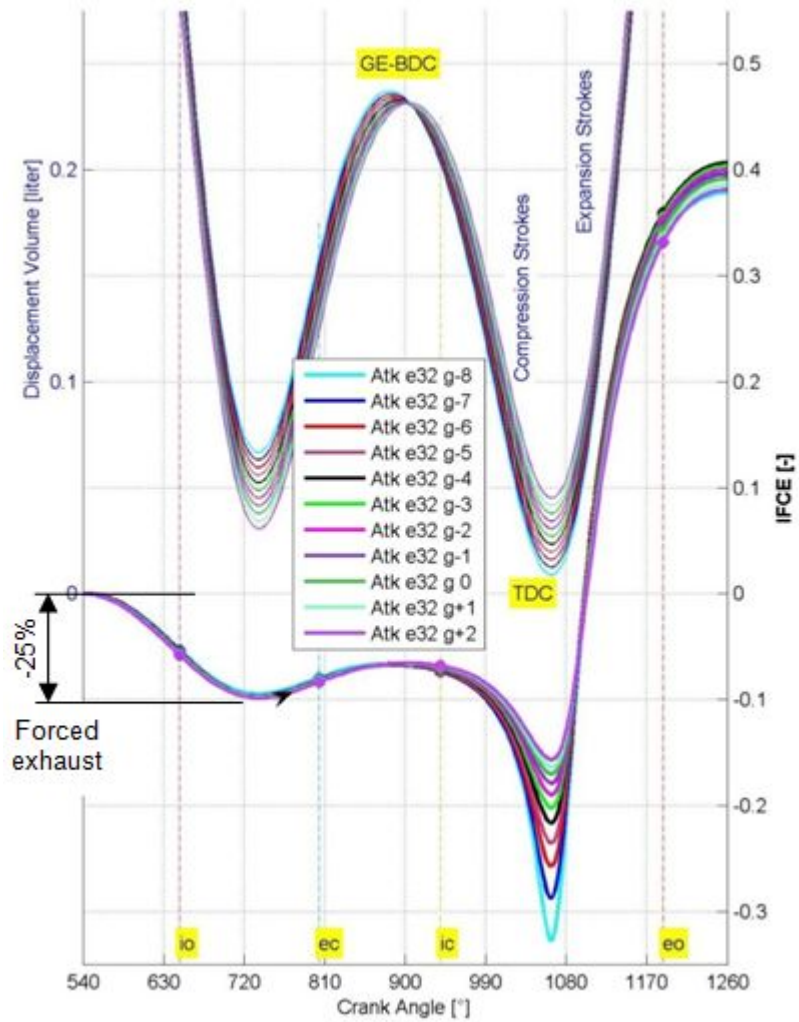
Figure 11B IFCE - crank angle (**IFCE,CA**) with valve timing (left axis) and displacement volume - crank angle (**V,CA**) diagrams for all cycles. The forced exhaust diminishes IFCE cycle-**in**dependent.
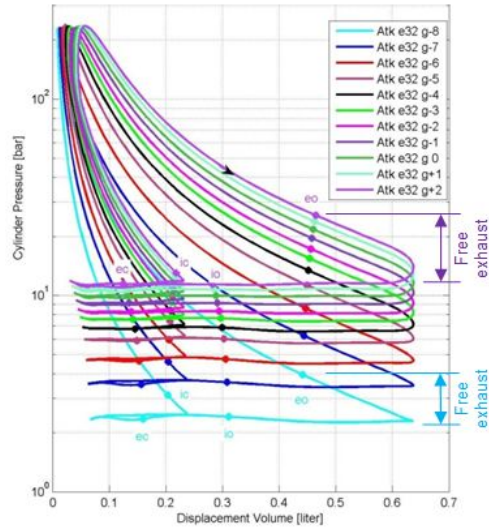
Figure 12B Cylinder pressure (logarithmic) - displacement volume (**p,V**) diagrams with valves timing for all cycles
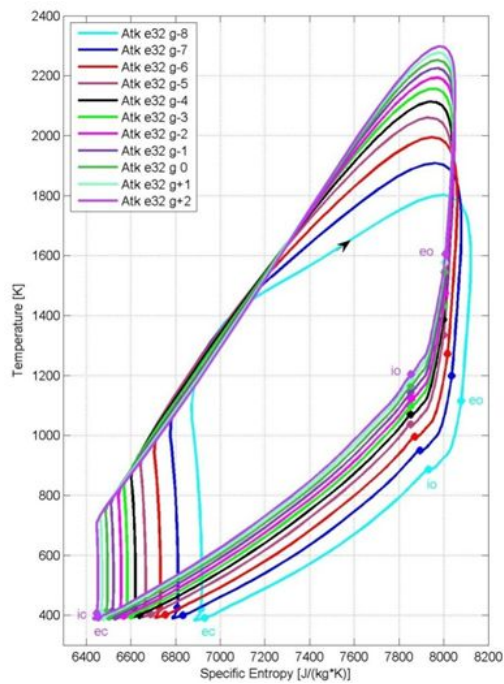

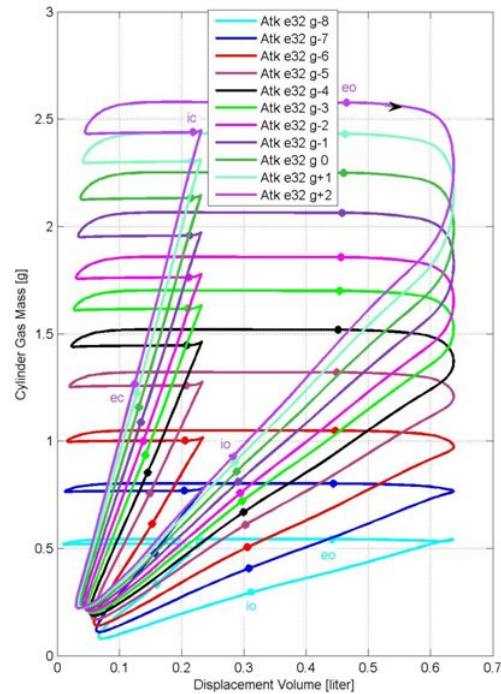**Figure 13B** Temperature - specific entropy (**T,s**) diagrams with valves timing for all cycles

Figure 14B Gas mass - displacement volume (**m,V**) diagrams with valves timing for all cycles

3. Conclusion

The implementation of real Atkinson cycles for turbocharged engines using asymmetrical crank mechanisms offers the following advantages: a) relatively high IMEP, b) higher IFCE leading to few CO2 emissions and c) lower temperatures during the combustion stage leading to few NOx emissions.

In order to achieve these performances, the engine requires the use of turbocharger systems with at least two stages which must be adapted accordingly and controlled with the help of bypasses to maximize their performance.

The optimum ratio between the internal (i.e. within the cylinder) and external (i.e. within turbines) expansion of the exhaust gases which maximize IFCE is reached when the VCR is close to 50% of VER.

An asymmetrical crank mechanism where the VCR may also be varied makes it possible to realize Atkinson cycles for part and full load even with stoichiometric AFR and without throttling.

References

[1] R. Weinowski, A. Sehr, S. Wedowski, S. Heuer, T. Hamm, C. Tiemann, *Future downsizing of S.I. engines - potentials and limits of 2- and 3-cylinder concepts*, Vienna Motor Symposium 2009, Austria

[2] V. Korte, G. Lumsden, N. Fraser, J. Hall, *30% higher efficiency at 50% less displacement*, MTZ 2010

[3] V. Gheorghiu, *CO2-Emission Reduction by Means of Enhancing the Thermal Conversion Efficiency of ICE Cycles,* SAE International Powertrains, Fuels & Lubricants Congress 2010, 10-SFL214-0032, Rio de Janeiro, Brazil

[4] Schutting, E, Neureiter, A, Fuchs, Ch., Schwarzenberger, T, Klell, M, Eichlseder, H, Kammerdiener, T, *Miller- and Atkinson-Cycle for Supercharged Diesel Engines*, MTZ 06 / 2007 (German)

[5] V. Gheorghiu, *Enhancement Potential of the Thermal Conversion Efficiency of ICE Cycles by Using of a real Atkinson Cycle Implementation and (Very) High Pressure Turbocharging*, ESDA International Automotive Congress, July 2010, Istanbul, Turkey